Letter

Distinct sequential and massive transfer processes for production of neutron-rich $N \approx 126$ nuclei in $^{238}\mathrm{U} + ^{198}\mathrm{Pt}$ reactions

K. Zhao,[1,2,*] Z. Liu,[3,4,†] F. S. Zhang,[5,6,7] N. Wang,[2,8] and J. Z. Duan[3]

[1]*Department of Nuclear Physics, China Institute of Atomic Energy, Beijing 102413, People's Republic of China*
[2]*Guangxi Key Laboratory of Nuclear Physics and Nuclear Technology, Guangxi Normal University, Guilin 541004, People's Republic of China*
[3]*Key Laboratory of High Precision Nuclear Spectroscopy, Institute of Modern Physics, Chinese Academy of Sciences, Lanzhou 730000, People's Republic of China*
[4]*School of Nuclear Science and Technology, University of Chinese Academy of Sciences, Beijing 100049, People's Republic of China*
[5]*Key Laboratory of Beam Technology of Ministry of Education, College of Nuclear Science and Technology, Beijing Normal University, Beijing 100875, People's Republic of China*
[6]*Institute of Radiation Technology, Beijing Academy of Science and Technology, Beijing 100875, People's Republic of China*
[7]*Center of Theoretical Nuclear Physics, National Laboratory of Heavy Ion Accelerator of Lanzhou, Lanzhou 730000, People's Republic of China*
[8]*Department of Physics, Guangxi Normal University, Guilin 541004, People's Republic of China*

(Received 11 April 2022; accepted 20 July 2022; published 29 July 2022)

To investigate the underlying mechanisms responsible for the enhanced production of new neutron-rich $N \approx 126$ nuclei in the reaction $^{238}\mathrm{U} + ^{198}\mathrm{Pt}$, detailed simulations of the system at an incident energy of 8 MeV/nucleon using the improved quantum molecular dynamics model have been performed. Sequential and massive transfer processes, responsible for the production of targetlike and projectilelike n-rich $N \approx 126$ fragments, respectively, have been recognized. Compared to sequential transfer, the contribution from the massive transfer process plays an almost equal role for the production of new nuclei with atomic number $Z \leqslant 76$. The two processes show distinct features in the angular and kinetic energy distributions in the laboratory system and hopefully can be disentangled experimentally.

DOI: 10.1103/PhysRevC.106.L011602

The properties of neutron-rich $N \approx 126$ nuclei are essential for understanding the astrophysical r-process abundance peak around $A = 195$ [1] and the evolution of the $N = 126$ neutron shell closure far from the β-stability line [2,3]. Multinucleon transfer (MNT) reaction has been proposed as an alternative approach of great potential to synthesize these $N = 126$ r-process waiting-point nuclei [4,5]. Considering that the ground-state Q values favor the transfer of protons from lead to xenon in the reaction $^{136}\mathrm{Xe} + ^{208}\mathrm{Pb}$, Zagrebaev and Greiner proposed to take advantage of the stabilizing effects of the neutron closed shells at $N = 82$ for ^{136}Xe and $N = 126$ for ^{208}Pb to enhance the production of $N \approx 126$ isotones below ^{208}Pb [4]. However, no evidence for such multiproton transfer was found in the experiments performed at Dubna and Argonne [6,7]. The GRAZING code calculations showed a significant advantage of the system $^{136}\mathrm{Xe} + ^{198}\mathrm{Pt}$ over $^{136}\mathrm{Xe} + ^{208}\mathrm{Pb}$ for producing new $N = 126$ isotopes because of larger neutron transfer probability compared to proton [8]. In the experiment of $^{136}\mathrm{Xe} + ^{198}\mathrm{Pt}$ at the incident energy of ≈ 8 MeV/nucleon performed at GANIL [9], the cross sections for $N = 126$ isotones were deduced and MNT reactions showed an obvious advantage over the fragmentation of the ^{208}Pb beam on the Be target [10] in the production of very neutron-rich nuclei with proton number $Z \leqslant 77$. MNT reactions between symmetric massive nuclei, such as ^{204}Hg with ^{198}Pt and ^{208}Pb, were performed at Argonne [11,12]. Rather neutron-rich transfer products were populated but no new isotopes in this region were observed up to now.

The dynamical processes involved in the MNT reactions attracted much interest in theoretical studies using different approaches. The effects of dynamical deformation on the potential energy surface and the mass distribution were investigated in the dinuclear system (DNS) framework [13–15]. In the calculations performed with the improved quantum molecular dynamics (ImQMD) model, the energy dissipation in the $^{136}\mathrm{Xe} + ^{198}\mathrm{Pt}$ system was found to be strongly associated with the incident energy [16]. In the stochastic mean-field approach, the mass distribution of primary fragments and the production of isotopes heavier than the target in the multinucleon transfer of $^{136}\mathrm{Xe} + ^{208}\mathrm{Pb}$

*zhaokai@ciae.ac.cn
†liuzhong@impcas.ac.cn

were better reproduced by considering the quantal diffusion mechanism [17,18].

The reaction between ^{238}U and ^{198}Pt was initially suggested as an alternative for the production of $N \approx 126$ neutron-rich nuclei by Zagrebaev and Greiner [19]. The calculated production cross sections for these neutron-rich nuclei were on average higher than those in the collision of ^{136}Xe with ^{208}Pb or ^{198}Pt by the Langevin approach [19] and the DNS model [20]. And such cross-section enhancement was confirmed by our recent calculations using the ImQMD model [21]. Due to the complicated dynamical processes involved, such as the coupling of single-particle and collective degrees of freedom, sequential nucleon transfer was assumed to play a main role in mass rearrangement in the Langevin approach [19], and only one nucleon transfer was considered in the DNS model [20]. Compared to the single-nucleon transfer, the transfer of massive clusters was proposed and supported by the observed large cross sections for the production of heavier actinides in Ref. [22]. The sequential transfer and the simultaneous transfer of several nucleons were also discussed based on the experimental measurements of reactions with the target ^{232}Th [23,24]. However, the detailed dynamical mechanisms of two transfer processes and their effects on the production of primary fragments are still unclear.

In the investigation of the underlying mechanism responsible for the favored production of neutron-rich $N \approx 126$ species in the reaction system $^{238}\mathrm{U} + {}^{198}\mathrm{Pt}$, the dynamical process of massive transfer is revealed by using the ImQMD model in the present work. In the model, a variety of degrees of freedom, such as neck formation, nucleon transfer, deformations of two colliding nuclei, and different types of separation of the composite system, can be considered simultaneously [25]. Over 3 000 000 events of the system $^{238}\mathrm{U} + {}^{198}\mathrm{Pt}$ are simulated at an incident energy of 8 MeV/nucleon and different impact parameters. At the initial time of reaction, the distance between the centers of mass of the projectile and the target is taken to be 30 fm. The decays of primary fragments produced in the ImQMD model are described by the statistical evaporation model (HIVAP code) [26,27]. A detailed description of the method of ImQMD + HIVAP can be found in Ref. [21].

Here we take the production of the primary fragment ^{204}Pt ($N = 126$) as an example and plot two different events at an impact parameter of $b = 6.0$ fm of the $^{238}\mathrm{U} + {}^{198}\mathrm{Pt}$ reaction at an incident energy of 8 MeV/nucleon in Fig. 1. They are the snapshots at three moments, namely, the touching of the projectile and the target, a moment in the multinucleon transfer process, and the reseparation of the composite system. Nucleons originated from the projectile and the target are represented in red and green, respectively. Event I presents a simple scenario where the targetlike fragment ^{204}Pt is produced by the transfer of six neutrons from the projectile to the target. Event II illustrates the transfer of a large number of nucleons from the projectile to the target. The remaining nucleons of the projectile ^{238}U and several nucleons transferred from the target ^{198}Pt form the primary projectilelike fragment ^{204}Pt in event II. In Fig. 1, the z axis is set as the beam direction and the x axis as the impact parameter. In the two cases, the pictures of the systems are quiet similar at the touching point, but very different at the reseparation of the composite systems. The fragment ^{204}Pt is produced along the trajectory of the target in event I, while it is produced along that of the projectile in event II.

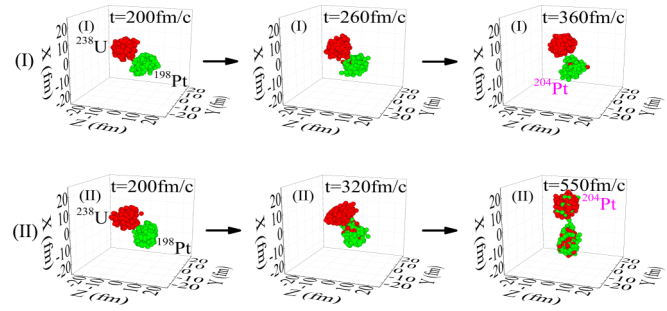

FIG. 1. The snapshots at three different moments of two examples producing primary fragments ^{204}Pt at an impact parameter of $b = 6.0$ fm in the $^{238}\mathrm{U} + {}^{198}\mathrm{Pt}$ reaction at an incident energy of 8 MeV/nucleon.

Figure 2 depicts the density along the axis of the system, which passes the centers of the projectilelike fragments (PLFs) and the targetlike fragments (TLFs), at different reaction times in the two events of Fig. 1. The neck region, having the smallest density between the two centers, is denoted in blue. In event I, the neck can be recognized easily as the density is always lower than 0.04 fm^{-3}, which is consistent with the picture of the sequential transfer of a few nucleons between two colliding nuclei. The neck position barely changed from the touching of the projectile and the target to the reseparation of the composite system. In event II, a bulky mass shifting from the projectile to the target with a high-density region over 0.14 fm^{-3} (denoted in red) occurs. It corresponds to the collective transfer of a large number of nucleons. It results in the shift of the neck region by about 4 fm towards the projectile in a short time. Therefore, two completely different dynamical processes are revealed in events I and II, leading to the production of the same primary fragment ^{204}Pt.

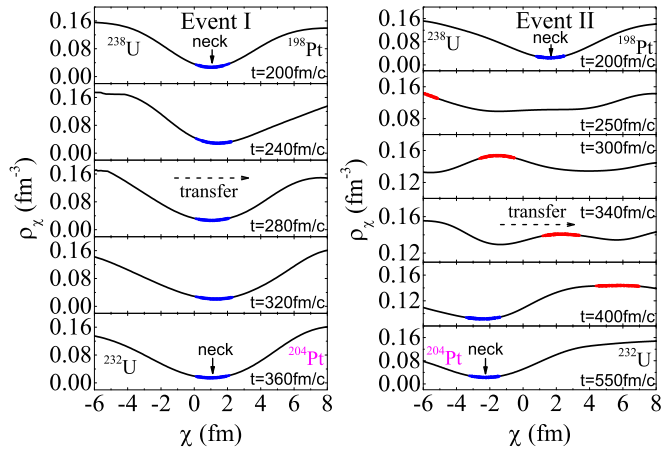

FIG. 2. The density evolution around the neck region for the two events shown in Fig. 1. The density is calculated along the axis of the system, which passes the centers of the PLFs and the TLFs.

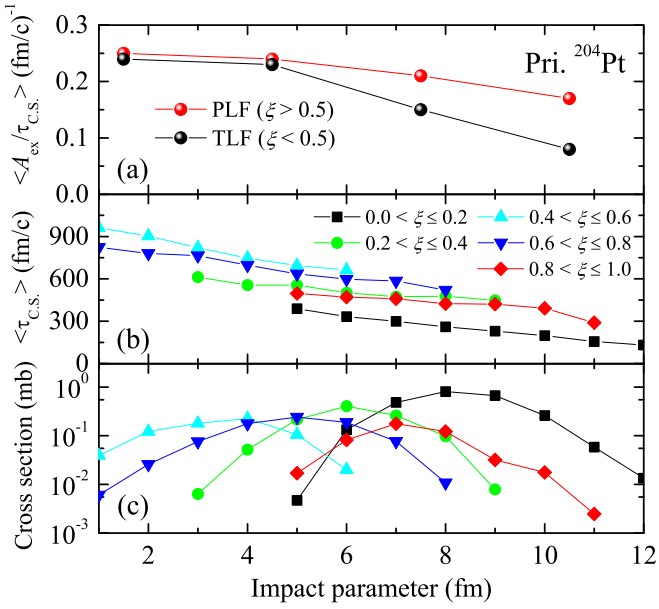

FIG. 3. (a) The nucleon exchange rates, (b) the average lifetimes of the composite systems (c.s.), and (c) the cross sections for producing the primary fragment ^{204}Pt as a function of impact parameters for different ξ groups.

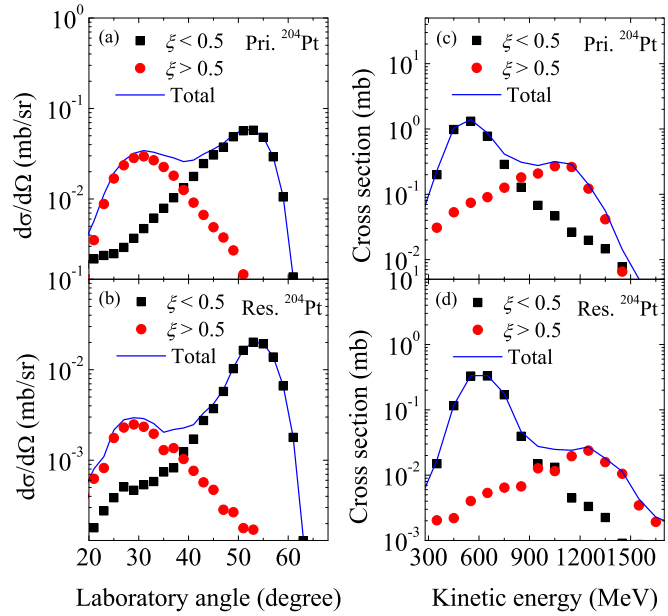

FIG. 4. The angular distributions of (a) primary and (b) residual fragments of ^{204}Pt produced in the ^{238}U + ^{198}Pt system at 8 MeV/nucleon in the laboratory system. Panels (c) and (d) present the distributions of kinetic energies of primary and residual ^{204}Pt, respectively.

In most events, the primary fragment ^{204}Pt is produced by the exchange of nucleons between the projectile and the target in both directions. To investigate the feature of the production mechanisms of primary fragments, we define a variable to describe the extent of nucleon transfer as $\xi = A_F^P/A_F$, where A_F is the mass number of the fragment and A_F^P is the number of nucleons coming from the projectile in this fragment. We take $A_{ex}/\tau_{c.s.}$ as the nucleon exchange rate, i.e., the average number of exchanged nucleons per unit time, where A_{ex} is the total number of nucleons exchanged between the projectile and the target. $\tau_{c.s.}$ is the lifetime of the composite system (c.s.), which is defined as the time interval between touching of two colliding nuclei and reseparation of the composite system. Figure 3 displays the average values of $A_{ex}/\tau_{c.s.}$, $\tau_{c.s.}$, and the corresponding production cross sections for the primary fragment ^{204}Pt. They are grouped according to ξ values as functions of the impact parameters. As shown in Fig. 3(a), the nucleon exchange rates for the production of PLFs ($\xi > 0.5$) and TLFs ($\xi < 0.5$) at large impact parameters are very different: the former is almost twice the latter. As the impact parameter decreases, the nucleon exchange rates for both increase and saturate to nearly an identical value. It is noted that the production of the ^{204}Pt PLFs requires the net transfer of 34 nucleons, while only 6 nucleons are required for the production of the ^{204}Pt TLFs. In Fig. 3(b), the average lifetimes of the composite systems for five groups of ξ decrease monotonically with increasing the impact parameter. The longest corresponds to the central collision where more nucleons are exchanged, while the shortest corresponds to peripheral collisions where the primary fragments are produced as either TLFs with the smallest ξ or PLFs with the largest ξ. For TLFs of $\xi < 0.5$, they can be understood by the sequential transfer of nucleons between two colliding nuclei. The transfer of more nucleons needs a longer lifetime of the composite system and generally occurs at smaller impact parameters. The group with the largest ξ (PLFs are denoted by red diamonds) is produced at similar impact parameters with the smallest ξ group (TLFs are denoted by black squares). In these PLFs, at least 34 nucleons are transferred from the projectile ^{238}U to the target for producing the primary fragment ^{204}Pt. The sequential transfer of nucleons cannot explain the short lifetime of the composite system denoted by the red diamonds. As Fig. 2 shows, large mass collective transfer plays a critical role in both the production of these PLFs and the evolution of the corresponding composite system. In Fig. 3(c), the production cross-section curve has a parabolalike shape for each group. The biggest contribution comes from TLFs produced in peripheral collisions at large impact parameters.

The different production mechanisms of ^{204}Pt in ^{238}U + ^{198}Pt revealed above are also present in the distributions of emitting angles and kinetic energies. In Fig. 4, we divide the production processes of ^{204}Pt into two groups, i.e., PLFs with $\xi > 0.5$ and TFLs with $\xi < 0.5$. Figures 4(a) and 4(b) illustrate the angular distributions of primary and residual ^{204}Pt fragments by blue lines in the laboratory system. For both primary and residual fragments, two peaks located at 30° and 53° come from the PLFs and TLFs, respectively. The distributions of kinematic energies in the laboratory system are shown in Figs. 4(c) and 4(d). The PLF and TLF components are also distinguishable, corresponding to the two bumps at about 1200 and 600 MeV.

Similar behavior is also found in the angular distributions of new isotopes of Os, Re, W, and Ta (see Fig. 5). Open

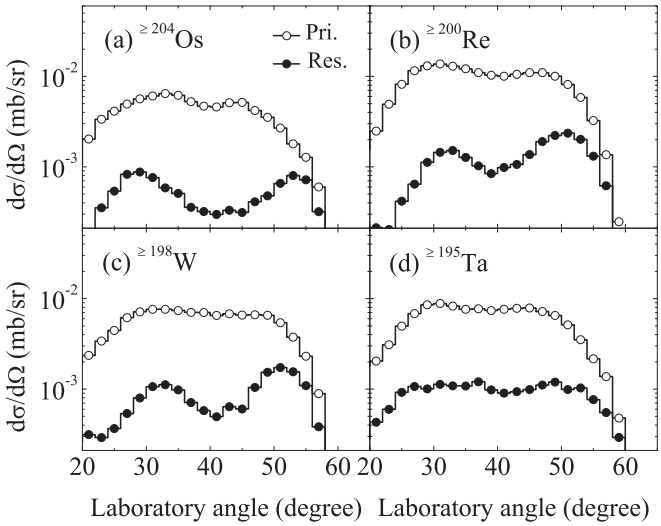

FIG. 5. The angular distributions of new isotopes in primary and residual fragments of elements (a) Os, (b) Re, (c) W, and (d) Ta in the laboratory system.

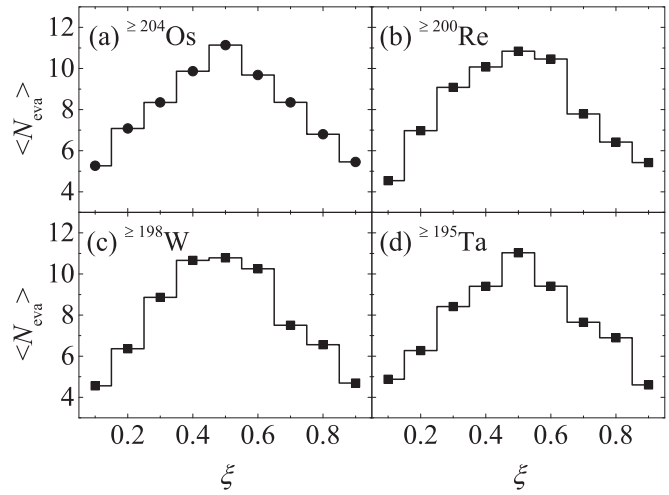

FIG. 7. The distributions of the average number of neutrons evaporated from primary fragments of (a) Os, (b) Re, (c) W, and (d) Ta.

and solid symbols represent primary and residual fragments, respectively. For new neutron-rich isotopes with lower atomic number, the contributions of the PLFs are significantly enhanced relative to TLFs compared to ^{204}Pt. However, the two peaks get closer to each other with decreasing atomic number and are less distinguishable for neutron-rich Ta isotopes. The production cross sections for these residual fragments depend on the cross sections for primary fragments and their excitation energies. Figure 6 shows the average excitation energies of the primary fragments as a function of ξ. The excitation energies of primary fragments peak around $\xi = 0.5$, corresponding to central collisions with the maximum number of nucleons exchanged and the longest lifetime of the composite system. The smallest and largest ξ values corresponding to peripheral collisions induce lower excitation energies. This is consistent with the correlation between the lifetime of the composite system and ξ shown in Fig. 3(b). In the case of a shorter lifetime, large mass collective transfer leads to lower excitation energies of primary fragments. The residual fragments of new neutron-rich nuclei are mainly produced by the evaporation of neutrons in the decay of the above primary fragments of Os, Re, W, and Ta. The average numbers of neutrons evaporated from per primary fragment of Os, Re, W, and Ta are presented in Fig. 7. Figure 7 shows a similar distribution to the excitation energies presented in Fig. 6. The largest excitation energies around $\xi = 0.5$ lead to the evaporation of more than ten neutrons. Fewer neutrons are evaporated in the decay of PLFs with larger ξ or TLFs with smaller ξ, both of which contribute to the survival of new neutron-rich nuclei. Figure 7 also indicates that the projectilelike fragments play a significantly important role in the production of these nuclei.

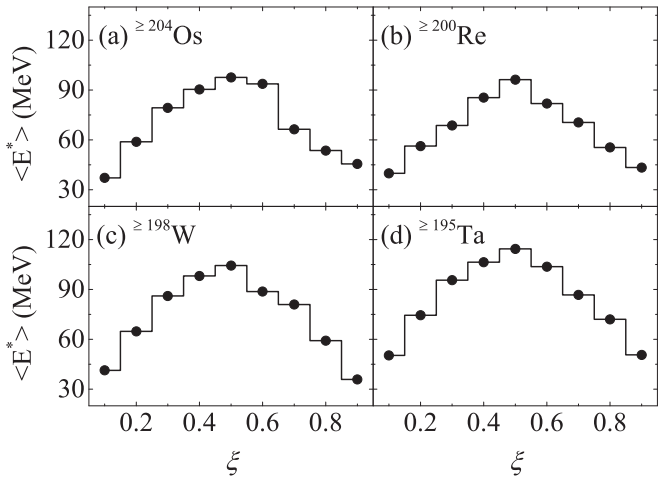

FIG. 6. The distributions of the average excitation energies of primary fragments of (a) Os, (b) Re, (c) W, and (d) Ta.

To summarize, the underlying mechanism responsible for the enhanced production of neutron-rich $N \approx 126$ nuclei with $Z \leqslant 78$ in the reaction $^{238}\mathrm{U} + ^{198}\mathrm{Pt}$ at an incident energy of 8 MeV/nucleon has been investigated by using the ImQMD model. In addition to TLFs, the contribution from PLFs to the production cross sections for these fragments has been found. Distinct dynamical processes are revealed in the production of PLFs and TLFs. Sequential transfer of nucleons plays a key role in producing TLFs, while massive transfer of nucleons plays a key role in producing PLFs. The difference between them manifests itself not only in the dynamical processes but also in the angular and kinetic energy distributions. The latter originated from PLF and TLF components can be distinguished in the experimental measurements.

The work is supported by the National Natural Science Foundation of China under Grants No. 11675266, No. 12135004, No. 11635003, No. 11961141004, No. U1867212, 11790325, and No. 11965004; the Continuous Basic Scientific Research Project No. WDJC-2019-13, Grant No.

BJ20002501; the Leading Innovation Project under Grants No. LC192209000701 and No. LC202309000201; the Open Project of Guangxi Key Laboratory of Nuclear Physics and Nuclear Technology under Grant No. NLK2020-01; the National Key R&D Program of China (Contract No. 2018YFA0404402), and the Strategic Priority Research Program of Chinese Academy of Sciences under Grant No. XDB34000000. We also acknowledge support by the Supercomputer Center of HIRFL at the Institute of Modern Physics of China.

[1] H. Grawe, K. Langanke, and G. Martínez-Pinedo, Nuclear structure and astrophysics, Rep. Prog. Phys. **70**, 1525 (2007).

[2] O. Sorlin and M.-G. Porquet, Nuclear magic numbers: New features far from stability, Prog. Part. Nucl. Phys. **61**, 602 (2008).

[3] F. Käppeler, F.-K. Thielemann, M. Wiescher, Current quests in nuclear astrophysics and experimental approaches, Annu. Rev. Nucl. Part. Sci. **48**, 175 (1998).

[4] V. Zagrebaev and W. Greiner, Production of New Heavy Isotopes in Low-Energy Multinucleon Transfer Reactions, Phys. Rev. Lett. **101**, 122701 (2008).

[5] W. D. Loveland, The synthesis of new neutron-rich heavy nuclei, Front. Phys. **7**, 23 (2019).

[6] E. M. Kozulin, E. Vardaci, G. N. Knyazheva, A. A. Bogachev, S. N. Dmitriev, I. M. Itkis, M. G. Itkis, A. G. Knyazev, T. A. Loktev, K. V. Novikov, E. A. Razinkov, O. V. Rudakov, S. V. Smirnov, W. Trzaska, and V. I. Zagrebaev, Mass distributions of the system ^{136}Xe + ^{208}Pb at laboratory energies around the Coulomb barrier: A candidate reaction for the production of neutron-rich nuclei at $N = 126$, Phys. Rev. C **86**, 044611 (2012).

[7] J. S. Barrett, W. Loveland, and R. Yanez, S. Zhu, A. D. Ayangeakaa, M. P. Carpenter, J. P. Greene, R. V. F. Janssens, T. Lauritsen, E. A. McCutchan, A. A. Sonzogni, C. J. Chiara, J. L. Harker, and W. B. Walters, ^{136}Xe + ^{208}Pb reaction: A test of models of multinucleon transfer reactions, Phys. Rev. C **91**, 064615 (2015).

[8] R. Yanez and W. Loveland, Predicting the production of neutron-rich heavy nuclei in multinucleon transfer reactions using a semi-classical model including evaporation and fission competition, GRAZING-F, Phys. Rev. C **91**, 044608 (2015).

[9] Y. X. Watanabe, Y. H. Kim, S. C. Jeong, Y. Hirayama, N. Imai, H. Ishiyama, H. S. Jung, H. Miyatake, S. Choi, J. S. Song, E. Clement, G. de France, A. Navin, M. Rejmund, C. Schmitt, G. Pollarolo, L. Corradi, E. Fioretto, D. Montanari, M. Niikura *et al.*, Pathway for the production of neutron-rich isotopes around the $N = 126$ shell closure, Phys. Rev. Lett. **115**, 172503 (2015).

[10] T. Kurtukian-Nieto, J. Benlliure, K.-H. Schmidt, L. Audouin, F. Becker, B. Blank, E. Casarejos, F. Farget, M. Fernández-Ordóñez, J. Giovinazzo, D. Henzlova, B. Jurado, J. Pereira, and O. Yordanov, Production cross sections of heavy neutron-rich nuclei approaching the nucleosynthesis *r*-process path around $A = 195$, Phys. Rev. C **89**, 024616 (2014).

[11] T. Welsh, W. Loveland, R. Yanez, J. S. Barrett, E. A. McCutchan, A. A. Sonzogni, T. Johnson, S. Zhu, J. P. Greene, A. D. Ayangeakaa, M. P. Carpenter, T. Lauritsen, J. L. Harker, W. B. Walters, B. M. S. Amro, and P. Copp, Modeling multinucleon transfer in symmetric collisions of massive nuclei, Phys. Lett. B **771**, 119 (2017).

[12] V. V. Desai, A. Pica, W. Loveland, J. S. Barrett, E. A. McCutchan, S. Zhu, A. D. Ayangeakaa, M. P. Carpenter, J. P. Greene, T. Lauritsen, R. V. F. Janssens, B. M. S. Amro, and W. B. Walters, Multinucleon transfer in the interaction of 977 MeV and 1143 MeV ^{204}Hg with ^{208}Pb, Phys. Rev. C **101**, 034612 (2020).

[13] Z. Q. Feng, Production of neutron-rich isotopes around $N = 126$ in multinucleon transfer reactions, Phys. Rev. C **95**, 024615 (2017).

[14] L. Zhu, P. W. Wen, C. J. Lin, X. J. Bao, J. Su, C. Li, and C. C. Guo, Shell effects in a multinucleon transfer process, Phys. Rev. C **97**, 044614 (2018).

[15] S. Q. Guo, X. J. Bao, H. F. Zhang, J. Q. Li, and N. Wang, Effect of dynamical deformation on the production distribution in multinucleon transfer reactions, Phys. Rev. C **100**, 054616 (2019).

[16] C. Li, X. X. Xu, J. J. Li, G. Zhang, B. Li, C. A. T. Sokhna, Z. S. Ge, F. Zhang, P. W. Wen, and F. S. Zhang, Production of new neutron-rich heavy nuclei with $Z = 56$–80 in the multinucleon transfer reactions of ^{136}Xe + ^{198}Pt, Phys. Rev. C **99**, 024602 (2019).

[17] S. Ayik, B. Yilmaz, O. Yilmaz, and A. S. Umar, Quantal diffusion approach for multinucleon transfers in Xe + Pb collisions, Phys. Rev. C **100**, 014609 (2019).

[18] S. Ayik, O. Yilmaz, B. Yilmaz, and A. S. Umar, Heavy-isotope production in ^{136}Xe + ^{208}Pb collisions at $E_{\mathrm{c.m.}} = 514$ MeV, Phys. Rev. C **100**, 044614 (2019).

[19] V. Zagrebaev and W. Greiner, Production of heavy trans-target nuclei in multinucleon transfer reactions, Phys. Rev. C **87**, 034608 (2013).

[20] L. Zhu, C. Li, J. Su, C. C. Guo, and W. Hua, Advantages of the multinucleon transfer reactions based on ^{238}U target for producing neutron-rich isotopes around $N = 126$, Phys. Lett. B **791**, 20 (2019).

[21] K. Zhao, Z. Liu, F. S. Zhang, and N. Wang, Production of neutron-rich $N = 126$ nuclei in multinucleon transfer reactions: Comparison between ^{136}Xe + ^{198}Pt and ^{238}U + ^{198}Pt reactions, Phys. Lett. B **815**, 136101 (2021).

[22] M. T. Magda and J. D. Leyba, Production of heavy elements by transfer of massive clusters, Int. J. Mod. Phys. E **01**, 221 (1992), and references therein.

[23] J. F. C. Cocks, P. A. Butler, K. J. Cann, P. T. Greenlees, G. D. Jones, J. F. Smith, P. M. Jones, R. Julin, S. Juutinen, D. Müller, M. Piiparinen, A. Savelius, R. Broda, B. Fornal, I. Ahmad, D. J. Blumenthal, M. P. Carpenter, B. Crowell, R. V. F. Janssens, T. L. Khoo, *et al.*, Multi-nucleon transfer reactions as a tool for spectroscopy of heavy nuclei, J. Phys. G: Nucl. Part. Phys. **26**, 23 (2000).

[24] D. C. Biswas, R. K. Choudhury, D. M. Nadkarni, and V. S. Ramamurthy, Evidence of massive cluster transfers in ^{19}F + ^{232}Th reaction at near barrier energies, Phys. Rev. C **52**, R2827 (1995).

[25] Y. X. Zhang, N. Wang, Q. F. Li, L. Ou, J. L. Tian, M. Liu, K. Zhao, X. Z. Wu, and Z. X. Li, Progress of quantum molecular

dynamics model and its applications in heavy ion collisions, Front. Phys. **15**, 54301 (2020).

[26] C. W. Shen, G. Kosenko, and Y. Abe, Two-step model of fusion for the synthesis of superheavy elements, Phys. Rev. C **66**, 061602(R) (2002).

[27] W. Reisdorf, F. P. Hessberger, K. D. Hildenbrand, S. Hofmann, G. Münzenberg, K.-H. Schmidt, W. F. W. Schneider, K. Sümmerer, G. Wirth, J. V. Kratz, K. Schutt, and C.-C. Sahm, Fusability and fissionability in ^{86}Kr-induced reactions near and below the fusion barrier, Nucl. Phys. A **444**, 154 (1985).